OL Organic Letters

pubs.acs.org/OrgLett Letter

Ring-Fused 1,4-Dihydro[1,2,4]triazin-4-yls through Photocyclization

Paulina Bartos, Victor G. Young, Jr., and Piotr Kaszyński*

Cite This: *Org. Lett.* 2020, 22, 3835−3840 Read Online

ACCESS | Metrics & More | Article Recommendations | Supporting Information

ABSTRACT: Halogen lamp irradiation of benzo[*e*][1,2,4]triazines **2**[**X**] in CH_2Cl_2 solutions leads to planar ring-fused 1,4-dihydro-[1,2,4]triazin-4-yl radicals **1** through a novel, potentially general, cyclization mechanism. The scope and efficiency of the method were established for unsubstituted and *ortho*-substituted (X = NH_2, Br, NO_2) phenoxy, naphthyloxy, and quinolinoxy derivatives **2**[**X**]. The regioselectivity of **2**[**X**] photocyclization was rationalized with DFT computational methods. Radicals **1** were characterized by spectroscopic (UV−vis, EPR), electrochemical, and XRD methods.

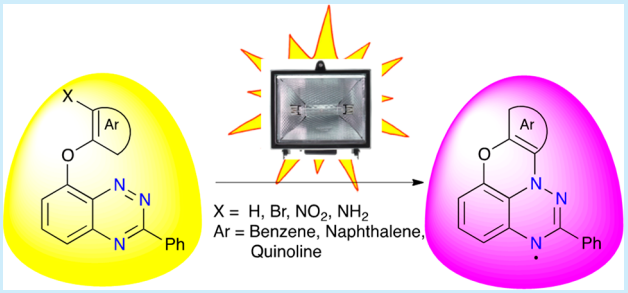

Benzo[*e*][1,2,4]triazin-4-yl radicals, such as the prototypical Blatter radical[1] (Figure 1) and its derivatives,[2] are becoming increasingly important structural elements for functional materials.[3] They have been explored in the context of controlled polymerization,[4] organic batteries,[5] molecular electronics,[6] near-IR sensing,[7] and magnetic[8,9] and spintronic applications[10,11] and have been studied as photoconductive liquid crystals.[12−15] Further progress in new functional materials and their applications depends, however, on advances in methods for construction of the 1,4-dihydro[1,2,4]triazin-4-yl ring and functional group transformations in its derivatives.

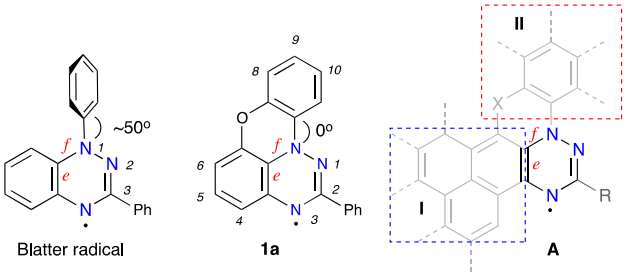

Figure 1. Structures of the Blatter radical, planar Blatter radical (**1a**), and a general structure for an extended polycyclic radical **A** formed by annulation of the 1,4-dihydro[1,2,4]triazin-4-yl unit (dark outline) at the *e* and *f* edges.

Two edges of the 1,4-dihydro[1,2,4]triazin-4-yl are available for ring fusion, and early synthetic efforts focused on the *e* edge (area **I** in **A**; Figure 1). A number of methods, including 6π electrocyclization,[1,16−22] reductive cyclocondensation,[22−24] azaphilic ArLi addition,[25] and postcyclization annulation[26−28] have been developed to construct polycyclic radicals. The resulting structures, such as the Blatter radical[1] as well as pyreno[*a*,*e*][1,2,4]triazin-4-yl[8,10,29] and thiazolo[5′,4′:4,5]-benzo[1,2-*e*][1,2,4]triazin-4-yl[27] derivatives, possess N(1)−aryl substituents with high torsion angles.[30] These substituents affect the molecular packing, intermolecular spin−spin interactions,[30] and stability of liquid crystalline phases.[12−15] Further expansion of the π system and greater control of the electronic properties of [1,2,4]triazinyl-based radicals is possible through simultaneous ring fusion at the *e* and *f* edges of the heterocyclic ring (areas **I** and **II** in **A**) and planarization of the entire structure, as shown in **1a** (Figure 1).

The concept of planar Blatter radicals was demonstrated recently[31] with e.g. **1a** (Figure 1). This exceptionally stable, 19π electron derivative was initially obtained in low (~25%) yield by intramolecular azaphilic cyclization of an organolithium derivative generated *in situ* from bromide **2a**[**Br**].[31] Recently, we developed a more efficient access to **1a** using a Pschorr-type radical cyclization starting with amine **2a**-[$\mathbf{NH_2}$].[32] These methods are much less useful for the synthesis of larger planar systems. Therefore, we focused on photochemical cyclization methods, such as the Mallory reaction,[33,34] which are widely used in preparation of closed-shell polycyclic aromatic systems,[35,36] including helicenes,[37] nanographenes,[38−40] photoswitches,[41] photochromic materials,[42,43] and π-extended corannulenes.[44−46]

Herein we report on a discovery of an unprecedented and potentially general method of photocyclization of 8-aryloxy benzo[*e*][1,2,4]triazines leading to planar Blatter radicals with extended π systems.

Exposure of solutions of nitro derivative **2a**[$\mathbf{NO_2}$] to sunlight resulted in formation of small amounts of radical **1a**.

Received: March 26, 2020
Published: April 24, 2020

https://dx.doi.org/10.1021/acs.orglett.0c01074
Org. Lett. 2020, 22, 3835−3840

Brief experimentations demonstrated that low concentration (~1 mM) degassed solutions in CH_2Cl_2 exposed to a 300 W halogen lamp work well, and after 12 h of irradiation radical **1a** was isolated in 31% or 98% yield, considering recovered, unconsumed starting **2a**[NO_2] (Figure 2).[47] Similar experiments with **2a**[**Br**] gave **1a** in higher yields (64%), while the unsubstituted **2a**[**H**] gave **1a** in 40% yield after 72 h of irradiation. Photocyclization reactions of 1-substituted 2-naphthyloxy derivatives **2b**[**X**] were more efficient. For instance, radical **1b** was isolated in 35% yield from **2b**[**Br**] after 3 h and in 55% from **2b**[NO_2] after 6 h (Figure 2). It was observed that **2b**[NO_2] was so photoreactive that it was difficult to work with it under ambient light conditions.

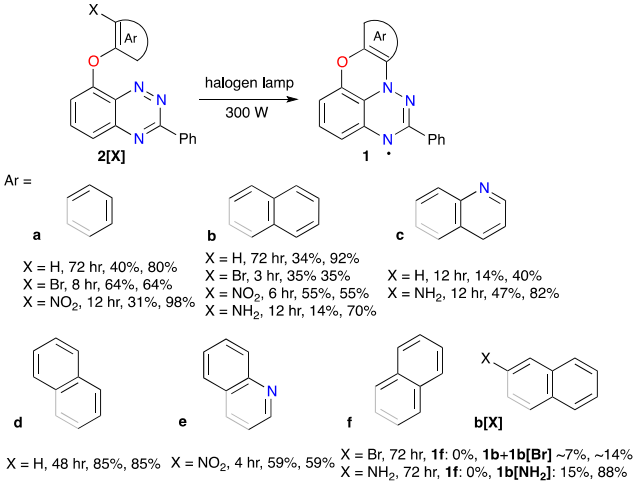

Figure 2. Photocyclization of **2**[**X**] to radicals **1**: *Method*: **2**[**X**] (300 mL CH_2Cl_2, $c \approx 1$ mM) is irradiated with a 300 W halogen lamp at 30−35 °C for 3−72 h in a Pyrex flask. Time, yields of isolated **1** and yields based on consumed **2**[**X**] are given.

Similar efficiency of cyclization was observed for 6-quinolinoxy derivatives **2c**[**H**] and **2c**[NH_2], for which **1c** was isolated in 14% and 47% yield, respectively, after 12 h of exposure to halogen lamp light. The yield was essentially the same in the presence of air. Irradiation of 1-naphthyloxy derivative **2d**[**H**] gave complete consumption of the staring material in 48 h, and radical **1d** was isolated in 85% yield. Extending the irradiation time did not significantly affect the yields presumably due to increased optical density of the solutions and possible photodegradation of the radicals. Similarly, high yields of **1e** were obtained by irradiation of 3-nitro-4-quinolinoxy derivative **2e**[NO_2] (Figure 2). In contrast, no expected radical **2f** was formed by irradiation of 3-bromo or 3-amino-2-naphthyloxy derivatives, **2f**[**Br**] and **2f**[NH_2]. Instead, the former gave a mixture of **1b**[**Br**] and **1b** in about 1:10 ratio, based on MS data, while the product of the latter precursor was isolated in a low yield and identified as **1b**[NH_2]. This selectivity for photocyclization at the naphthalene C(1) position suggests a possible route to functionalized derivatives. The desired radical **1f** was obtained in 14% yield by treatment of **2f**[**Br**] with *t*-BuLi and in 76% yield by thermolysis of *N*-nitrosoacetamide **2f**[**N(NO)Ac**] according to previous methods.[25,32] The aza-Pschorr method[32] did not yield radicals **1b** and **1c** using **2b**[**NHAc**] and **2c**[**NHAc**], respectively.

Comparative analysis of photocyclization products revealed complete selectivity in cyclization of **2a**[**X**] for the C(2) position, **2b**[**X**] and **2f**[**X**] for the C(1) position, and **2c**[**X**] for the analogous C(5) position. This is in full agreement with DFT computational results. Also in each reaction, only a single product, starting material, and intractable highly colored byproducts were observed. In the case of **2f**[**Br**], radical **1b**[**Br**] was accompanied by its debromination product **1b**.

The requisite precursors **2**[**H**], **2**[**Br**], and **2**[NH_2] were obtained from 8-fluoro-3-phenylbenzo[*e*][1,2,4]triazine[31] (**3**) by nucleophilic aromatic substitution reactions with appropriate *ortho*-substituted phenols **4**[**X**] in the presence of NaH (Scheme 1). Reactions of **3** with 2-nitro-1-naphthol (**4d**[NO_2]) did not yield the substitution product even at higher temperatures, presumably due to steric effects. Therefore, **2e**[NO_2] was obtained in a similar manner using 8-hydroxy-3-phenylbenzo[*e*][1,2,4]triazine (**5**) and nitro derivative **6e**[NO_2].

Scheme 1. Synthesis of Derivatives 2[**X**][a]

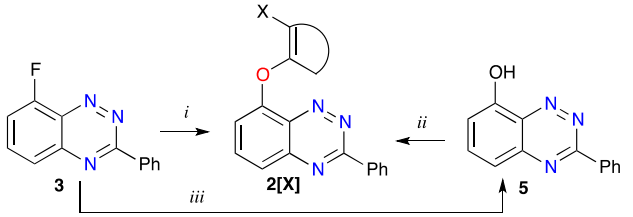

[a]Reagents and conditions: (*i*) *ortho*-substituted phenol **4**[**X**], 60% NaH, DMSO, 80 °C, 1−12 h; (*ii*) *ortho*-halo nitroarene **6**[NO_2], 60% NaH, DMSO, 80 °C, 1 h; (*iii*) [Bu_4N]$^+OH^-$, THF, 80 °C, 48 h.

For a better understanding of experimental results, photocyclization of model derivatives ***2[X]***, in which the C(3)−Ph group is replaced with a hydrogen atom, was modeled at the (TD)CAM-B3LYP/6-31G(d,p) level of theory using a relaxed scan of the PES along the N(1)···C trajectory (e.g., Figure 3).[48]

Analysis of results indicates that the heights of the energy barrier to cyclization of ***2[X]*** in the S_1 state is lower for X = NH_2 and H than for X = NO_2. Results also demonstrate a strong preference for regioselective cyclization at the C(1) position of naphthalene in ***2b[X]*** and ***2f[X]*** (Figure 3) and for the C(5) position in 6-quinolinoxy derivatives ***2c[X]***. Inspection of the lowest energy excitations of ***2[X]*** shows that the observed regiochemistry of cyclization corresponds to the distribution of the excited state, and that the density of the π orbital localized on the aryloxy fragment could be used as a predictor of the cyclization mode (Figure 4).[48]

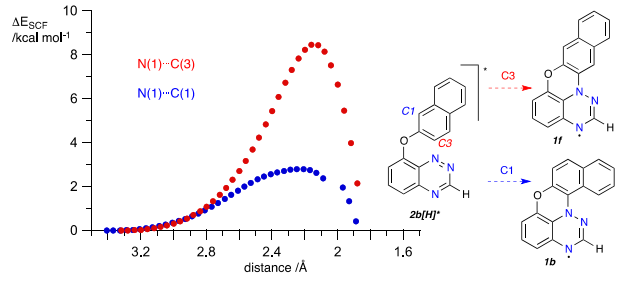

Figure 3. Relative energy of a PES relaxed scan along the N(1)···C(1) vector (blue), leading to ***1b***, and N(1)···C(3) vector (red), leading to ***1f***, in the S_1 state of model ***2b[H]****.

https://dx.doi.org/10.1021/acs.orglett.0c01074
Org. Lett. 2020, 22, 3835−3840

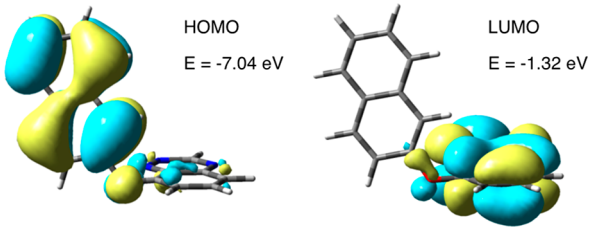

Figure 4. TD-DFT derived contours for FMOs of ***2b[H]*** involved in excitation calculated at 336 nm (f = 0.0154). Note the larger HOMO amplitude on naphthalene C(1) position than on the C(3).

Computational data revealed that the GS-to-GS transformation of ***2[X]*** to ***1***+X· is endothermic and the formation of ***1*** most likely occurs during the $S_1 \rightarrow S_0$ internal conversion and vibrational relaxation processes. TD-DFT calculations indicate that the initial vertical excitation is worth about 62−67 kcal mol^{-1} and the subsequent vibrational relaxation sets the relaxed excited ***2[X]**** at about 49−59 kcal mol^{-1} above the GS. This excess energy is sufficient to support homolysis of the weak C−X bond in the cyclized product and to yield ***1***+X·, as shown for **2**[**X**] in Figure 5. Thus, transformation of ***2[X]**** to ***1***+X· in the GS is moderately, for X = H, to highly exothermic, for X = NO_2, augmented by an increase of entropy. Fragment X· is presumably trapped by the solvent or oxidized by residual oxygen. Such a stabilization of the photocyclization reactive intermediate by formation of a stable radical has not been reported before.

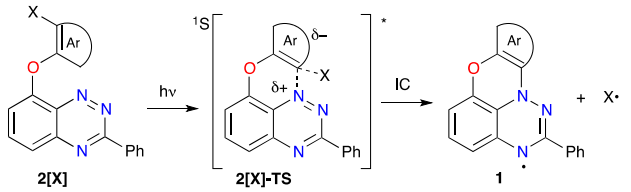

Figure 5. Proposed mechanism for the photochemical formation of **1** from **2**[**X**].

Photocyclization of aromatic compounds typically leads to dihydro derivatives, which may be stable valence isomers (e.g., photochromic fulgides and chromones)[41−43] and may require oxidation[33,34] or elimination of a small molecule (e.g., HX and H_2O)[35,49] to restore aromaticity or reduction.[35] To the best of our knowledge, the presently discovered process represents a new pathway of photocyclization of aromatic derivatives, in which stabilization of the photogenerated intermediate takes place through the formation of a stable radical.

The structure of **1f** was confirmed with the single crystal XRD analysis, which revealed two planar molecules in the asymmetric unit cell oriented at 85.7° angle to each other (Figure 6). The molecules form two independent evenly spaced slipped stacks with interplanar distances of 3.312 and 3.328 Å.

To assess the effect of π system extension in **1a** on electronic properties, radicals **1** were analyzed by spectroscopic (UV−vis and EPR) and electrochemical methods.

Comparison of **1a** with derivatives **1b**−**1f** demonstrate that extension of the π system has only a small effect on the absorption spectra. All radicals **1** exhibit low intensity broad absorption bands in the entire visible range (Figure 7).[48] The three main maxima located at about 550, 650, and 700 nm can

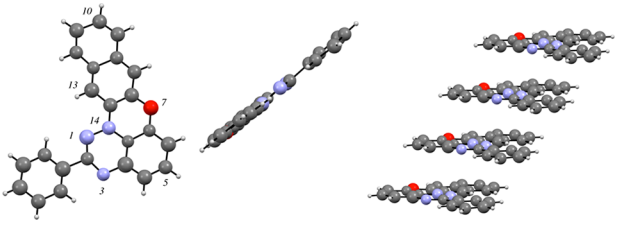

Figure 6. Left: Structural diagram for two unique molecules of **1f** in the asymmetric unit cell. Right: partial packing diagram. Selected intramolecular dimensions for molecule A: N(1)−N(14) = 1.42(2) Å, N(14)−C(13a) = 1.37(3) Å. For details see the Supporting Information (SI).

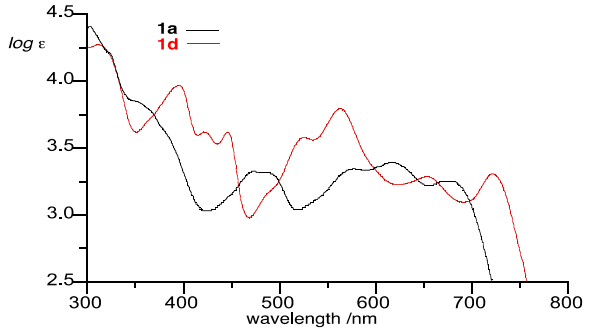

Figure 7. UV−vis spectra for radical **1a** (black) and **1d** (red) in CH_2Cl_2.

be ascribed mainly to the α-HOMO→ α-LUMO+1, α-HOMO→ α-LUMO, and β-HOMO→ β-LUMO transitions, respectively, on the basis of TD-DFT calculations.[48] The position of the lowest energy absorption band varies in a narrow range of ∼675 nm in **1a** and **1e** to 721 nm in **1d**, which corresponds to an optical band gap of 1.64−1.73 eV (Table 1).

Table 1. Cyclic Voltammetry Data,[a] Estimated Energy of the HOMO, and Optical Band Gap E_g for Radicals 1[a]

Radical	$E_{1/2}{}^{-1/0}$ (V)	$E_{1/2}{}^{0/+1}$ (V)	$E_{cell}{}^{b}$ (V)	$E_{HOMO}{}^{c}$ (eV)	$E_g{}^{d}$ (eV)
1a[e]	−0.86	0.31	1.16	−4.85	1.66
1b	−0.89	0.25	1.14	−4.80	1.67
1c	−0.83	0.31	1.14	−4.87	1.68
1d	−0.80	0.25	1.05	−4.80	1.64
1e	−0.78	0.36	1.14	−4.91	1.73
1f	−0.77	0.35	1.12	−4.90	1.69

[a]Potentials reported vs SCE. [b]$E_{cell} = E_{1/2}{}^{0/+1} - E_{1/2}{}^{-1/0}$. [c]Calculated from the onset of the oxidation wave: $E_{HOMO/LUMO} = -(E_{(onset\ ox/red\ vs\ Fc+/Fc)} + 5.1)$; ref 50. [d]Optical band gap. [e]From ref 32. For details, see the SI.

Similarly, extension of the π system by annulation of benzene ring to **1a** has a small effect on the redox potentials: annulation at the *ab* position of **1a** (Figure 8) shifts cathodically the $E_{1/2}{}^{0/+1}$ potential (−0.06 V in **1b**), annulation in the *bc* position affects mainly the $E_{1/2}{}^{-1/0}$ potential (+0.09 V in **1f**), and annulation in the *cd* position shifts both potentials by ±0.06 V narrowing the electrochemical window by 0.11 to 1.05 V in **1d** (Table 1). Redox potentials of quinoline derivatives **1c** and **1e** exhibit moderate anodic shifts relative to those of the naphthalene analogues.

Electron paramagnetic resonance spectroscopy (EPR) demonstrated that a_N *hfcc* values are similar for all radicals **1**

https://dx.doi.org/10.1021/acs.orglett.0c01074
Org. Lett. 2020, 22, 3835−3840

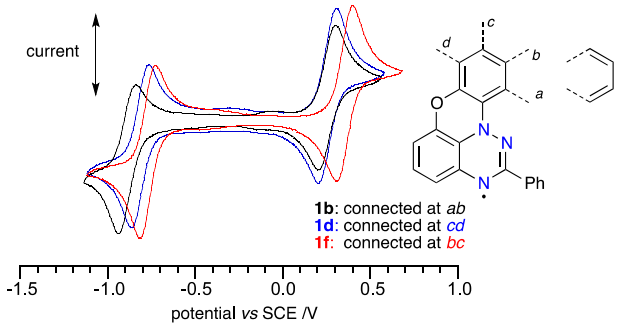

Figure 8. Cyclic voltammograms for radicals **1a** (black), **1d** (red), and **1h** (blue); 0.5 mM in CH_2Cl_2 $[n\text{-}Bu_4N]^+$ $[PF_6]^-$ (50 mM), at *ca.* 20 °C, 50 mV s^{-1}, glassy carbon working electrode.

(typically $a_N \approx 7.2$, 4.2, and 4.0 G) indicating again little effect of the π system extension.[48] Surprisingly, the Radical Delocalization Value,[51] RDV^{-1}, calculated with the DFT methods, suggests that the spin in π-expanded derivatives **1b**–**1f** (RDV^{-1} = 3.592–3.841) is no more delocalized than in the parent planar Blatter radical **1a** (RDV^{-1} = 3.858). The lower RDV^{-1} value for radicals **1b** (3.611) and **1c** (3.592) is consistent with lower spin delocalization, presumably due to their predicted nonplanar structures.

In summary, we have describe a new photochemical process, which through intramolecular cyclization of readily available precursors cleanly gives stable, π-delocalized polycyclic [1,2,4]triazinyl radicals. At the same time, this process constitutes a new method for construction of the benzo[*b*]-[1,4]oxazine ring.[52] The new method has been illustrated with five examples, which include radicals with 5 fused six-membered rings (21 sp^2 hybridized atoms) and 23π delocalized electrons. The reported photocyclization reaction occurs with high regioselectivity, which can be predicted with DFT methods. The method opens up new opportunities in synthesis of unprecedented paramagnetic functional materials and enables synthesis of well-defined extended π systems of type **A**.

■ ASSOCIATED CONTENT

Supporting Information

The Supporting Information is available free of charge at https://pubs.acs.org/doi/10.1021/acs.orglett.0c01074.

Preparative and analytical details, UV–vis and EPR spectra, electrochemical data, details of XRD analysis and computational results (PDF)

Accession Codes

CCDC 1990383 contains the supplementary crystallographic data for this paper. These data can be obtained free of charge via www.ccdc.cam.ac.uk/data_request/cif, or by emailing data_request@ccdc.cam.ac.uk, or by contacting The Cambridge Crystallographic Data Centre, 12 Union Road, Cambridge CB2 1EZ, UK; fax: +44 1223 336033.

■ AUTHOR INFORMATION

Corresponding Author

Piotr Kaszyński – *Faculty of Chemistry, University of Łódź, 91-403 Łódź, Poland; Centre of Molecular and Macromolecular Studies, Polish Academy of Sciences, 90-363 Łódź, Poland; Department of Chemistry, Middle Tennessee State University, Murfreesboro, Tennessee 37132, United States;* orcid.org/0000-0002-2325-8560; Email: PiotrK@cbmm.lodz.pl

Authors

Paulina Bartos – *Faculty of Chemistry, University of Łódź, 91-403 Łódź, Poland;* orcid.org/0000-0003-0514-951X

Victor G. Young, Jr. – *X-ray Crystallographic Laboratory, Department of Chemistry, University of Minnesota, Twin Cities, Minnesota 55455, United States*

Complete contact information is available at: https://pubs.acs.org/10.1021/acs.orglett.0c01074

Notes

The authors declare no competing financial interest.

■ ACKNOWLEDGMENTS

Support for this work was provided by the National Science Center (2017/25/B/ST5/02851) and Foundation for Polish Science (TEAM/2016-3/24). ChemMatCARS Sector 15 is supported by the NSF under Grant Number CHE-1834750. This research used resources of the Advanced Photon Source, a U.S. Department of Energy (DOE) Office of Science User Facility operated for the DOE Office of Science by Argonne National Laboratory under Contract No. DE-AC02-06CH11357. Authors thank Ms. Małgorzata Celeda for her technical assistance.

■ DEDICATION

Dedicated to Professor Josef Michl in honor of his 81st birthday.

■ REFERENCES

(1) Blatter, H. M.; Lukaszewski, H. A New Stable Free Radical. *Tetrahedron Lett.* **1968**, *9*, 2701–2705.

(2) Constantinides, C. P.; Koutentis, P. A. Stable N- and N/S-Rich Heterocyclic Radicals: Synthesis and Applications. *Adv. Heterocycl. Chem.* **2016**, *119*, 173–207.

(3) Ratera, I.; Veciana, J. Playing with organic radicals as building blocks for functional molecular materials. *Chem. Soc. Rev.* **2012**, *41*, 303–349.

(4) Demetriou, M.; Berezin, A. A.; Koutentis, P. A.; Krasia-Christoforou, T. Benzotriazinyl-mediated Controlled radical polymerization of styrene. *Polym. Int.* **2014**, *63*, 674–679.

(5) Häupler, B.; Schubert, U. S.; Wild, A.; Koutentis, P. A.; Zissimou, G. Verwendung benzotriazinyl-haltiger Polymere als Ladungsspeicher, DE 102017005924 A1, 27.12.2018.

(6) Bejarano, F.; Olavarria-Contreras, I. J.; Droghetti, A.; Rungger, I.; Rudnev, A.; Gutiérrez, D.; Mas-Torrent, M.; Veciana, J.; van der Zant, H. S. J.; Rovira, C.; Burzurí, E.; Crivillers, N. Robust Organic Radical Molecular Junctions Using Acetylene Terminated Groups for C–Au Bond Formation. *J. Am. Chem. Soc.* **2018**, *140*, 1691–1696.

(7) Zheng, Y.; Miao, M.-s.; Dantelle, G.; Eisenmenger, N. D.; Wu, G.; Yavuz, I.; Chabinyc, M. L.; Houk, K. N.; Wudl, F. A Solid-State Effect Responsible for an Organic Quintet State at Room Temperature and Ambient Pressure. *Adv. Mater.* **2015**, *27*, 1718–1723.

(8) Ciccullo, F.; Gallagher, N. M.; Geladari, O.; Chassé, T.; Rajca, A.; Casu, M. B. A Derivative of the Blatter Radical as a Potential Metal-Free Magnet for Stable Thin Films and Interfaces. *ACS Appl. Mater. Interfaces* **2016**, *8*, 1805–1812.

(9) Hu, X.; Chen, H.; Zhao, L.; Miao, M.; Zheng, Y. Observation of a Solid-State-Induced Thermally Populated Spin-Triplet State in Radical Regioisomers. *Chem. Mater.* **2019**, *31*, 10256–10262.

(10) Ciccullo, F.; Calzolari, A.; Bader, K.; Neugebauer, P.; Gallagher, N. M.; Rajca, A.; van Slageren, J.; Casu, M. B. Interfacing a Potential

Purely Organic Molecular Quantum Bit with a Real-Life Surface. *ACS Appl. Mater. Interfaces* **2019**, *11*, 1571−1578.
(11) Low, J. Z.; Kladnik, G.; Patera, L. L.; Sokolov, S.; Lovat, G.; Kumarasamy, E.; Repp, J.; Campos, L. M.; Cvetko, D.; Morgante, A.; Venkataraman, L. The Environment-Dependent Behavior of the Blatter Radical at the Metal−Molecule Interface. *Nano Lett.* **2019**, *19*, 2543−2548.
(12) Jasiński, M.; Szczytko, J.; Pociecha, D.; Monobe, H.; Kaszyński, P. Substituent-dependent magnetic behavior of discotic benzo[*e*]-[1,2,4]triazinyls. *J. Am. Chem. Soc.* **2016**, *138*, 9421−9424.
(13) Jasiński, M.; Szymańska, K.; Gardias, A.; Pociecha, D.; Monobe, H.; Szczytko, J.; Kaszyński, P. Tuning Magnetic Properties of Columnar Benzo[*e*][1,2,4]triazin-4-yls with the Molecular Shape. *ChemPhysChem* **2019**, *20*, 636−644.
(14) Jasiński, M.; Kapuściński, S.; Kaszyński, P. Stability of a columnar liquid crystalline phase in isomeric derivatives of the 1,4-dihydrobenzo[*e*][1,2,4]triazin-4-yl: conformational effects in the core. *J. Mol. Liq.* **2019**, *277*, 1054−1059.
(15) Kapuściński, S.; Gardias, A.; Pociecha, D.; Jasiński, M.; Szczytko, J.; Kaszyński, P. Magnetic behaviour of bent-core mesogens derived from the 1,4-dihydrobenzo[*e*][1,2,4]triazin-4-yl. *J. Mater. Chem. C* **2018**, *6*, 3079−3088.
(16) Neugebauer, F. A.; Umminger, I. Über 1,4-Dihydro-1,2,4-benzotriazinyl-Radikale. *Chem. Ber.* **1980**, *113*, 1205−1225.
(17) Koutentis, P. A.; Lo Re, D. Catalytic Oxidation of N-Phenylamidrazones to 1,3-Diphenyl-1,4-dihydro-1,2,4-benzotriazin-4-yls: An Improved Synthesis of Blatter's Radical. *Synthesis* **2010**, 2075−2079.
(18) Constantinides, C. P.; Koutentis, P. A.; Loizou, G. Synthesis of 7-aryl/heteraryl-1,3-diphenyl-1,2,4-benzotriazinyls via palladium catalyzed Stille and Suzuki-Miyaura reactions. *Org. Biomol. Chem.* **2011**, *9*, 3122−3125.
(19) Constantinides, C. P.; Koutentis, P. A.; Rawson, J. M. Antiferromagnetic Interactions in 1D Heisenberg Linear Chains of 7-(4-Fluorophenyl) and 7-Phenyl-Substituted 1,3-Diphenyl-1,4-dihydro- 1,2,4-benzotriazin-4-yl Radicals. *Chem. - Eur. J.* **2012**, *18*, 15433−15438.
(20) Miura, Y.; Yoshioka, N. π-Stacked structure of thiadiazolo-fused benzotriazinyl radical: Crystal structure and magnetic properties. *Chem. Phys. Lett.* **2015**, *626*, 11−14.
(21) Savva, A. C.; Mirallai, S. I.; Zissimou, G. A.; Berezin, A. A.; Demetriades, M.; Kourtellaris, A.; Constantinides, C. P.; Nicolaides, C.; Trypiniotis, T.; Koutentis, P. A. Preparation of Blatter Radicals via Aza-Wittig Chemistry: The Reaction of N-Aryliminophosphoranes with 1-(Het)aroyl-2-aryldiazenes. *J. Org. Chem.* **2017**, *82*, 7564−7575.
(22) Bodzioch, A.; Zheng, M.; Kaszyński, P.; Utecht, G. Functional Group Transformations in Derivatives of 1,4-Dihydrobenzo[1,2,4]-triazinyl Radical. *J. Org. Chem.* **2014**, *79*, 7294−7310.
(23) Berezin, A. A.; Zissimou, G.; Constantinides, C. P.; Beldjoudi, Y.; Rawson, J. M.; Koutentis, P. A. Route to benzo- and pyrido-fused 1,2,4-triazinyl radicals via N'-(het)aryl-N'-[2-nitro(het)aryl]-hydrazides. *J. Org. Chem.* **2014**, *79*, 314−327.
(24) Takahashi, Y.; Miura, Y.; Yoshioka, N. Introduction of Three Aryl Groups to Benzotriazinyl Radical by Suzuki-Miyaura Cross-Coupling Reaction. *Chem. Lett.* **2014**, *43*, 1236−1238.
(25) Constantinides, C. P.; Obijalska, E.; Kaszyński, P. Access to benzo[*e*][1,2,4]triazinyl derivtives. *Org. Lett.* **2016**, *18*, 916−919.
(26) Constantinides, C. P.; Berezin, A. A.; Manoli, M.; Leitus, G. M.; Zissimou, G.; Bendikov, M.; Rawson, J. M.; Koutentis, P. A. Structural, Magnetic, and Computational Correlations of Some Imidazolo-Fused 1,2,4-Benzotriazinyl Radicals. *Chem. - Eur. J.* **2014**, *20*, 5388−5396.
(27) Berezin, A. A.; Constantinides, C. P.; Drouza, C.; Manoli, M.; Koutentis, P. A. From Blatter Radical to 7-Substituted 1,3-Diphenyl-1,4-dihydrothiazolo[5′,4′:4,5]benzo[1,2-e][1,2,4]triazin-4-yls: Toward Multifunctional Materials. *Org. Lett.* **2012**, *14*, 5586−5589.
(28) Berezin, A. A.; Constantinides, C. P.; Mirallai, S. I.; Manoli, M.; Cao, L. L.; Rawson, J. M.; Koutentis, P. A. Synthesis and properties of imidazolo-fused benzotriazinyl radicals. *Org. Biomol. Chem.* **2013**, *11*, 6780−6795.
(29) Zheng, Y.; Miao, M.-s.; Kemei, M. C.; Seshadri, R.; Wudl, F. The Pyreno-Triazinyl Radical − Magnetic and Sensor Properties. *Isr. J. Chem.* **2014**, *54*, 774−778.
(30) Gardias, A.; Kaszyński, P.; Obijalska, E.; Trzybiński, D.; Domagała, S.; Woźniak, K.; Szczytko, J. Magnetostructural investigation of highly orthogonal 1-aryl-3-phenyl-1,4-dihydrobenzo[*e*]-[1,2,4]triazin-4-yl derivatives. *Chem. - Eur. J.* **2018**, *24*, 1317−1329.
(31) Kaszyński, P.; Constantinides, C. P.; Young, V. G., Jr. The Planar Blatter Radical: Structural Chemistry of 1,4-Dihydrobenzo[*e*]-[1,2,4]triazin-4-yls. *Angew. Chem., Int. Ed.* **2016**, *55*, 11149−11152.
(32) Bartos, P.; Anand, B.; Pietrzak, A.; Kaszyński, P. Functional Planar Blatter Radical through Pschorr-Type Cyclization. *Org. Lett.* **2020**, *22*, 180−184.
(33) Mallory, F. B.; Mallory, C. W. Photocyclization of stilbenes and related molecules. *Org. React.* **1984**, *30*, 1−456.
(34) Jørgensen, K. B. Photochemical Oxidative Cyclisation of Stilbenes and Stilbenoids—The Mallory-Reaction. *Molecules* **2010**, *15*, 4334−4358.
(35) De Keukeleire, D.; He, S. L. Photochemical strategies for the construction of polycyclic molecules. *Chem. Rev.* **1993**, *93*, 359−380.
(36) Begunov, R. S.; Ryzvanovich, G. A. Synthesis of pyrido[1,2-*a*]benzimidazoles and other fused imidazole derivatives with a bridgehead nitrogen atom. *Russ. Chem. Rev.* **2013**, *82*, 77−97.
(37) Hoffmann, N. Photochemical reactions applied to the synthesis of helicenes and helicene-like compounds. *J. Photochem. Photobiol., C* **2014**, *19*, 1−19.
(38) Mallory, F. B.; Butler, K. E.; Evans, A. C.; Brondyke, E. J.; Mallory, C. W.; Yang, C.; Ellenstein, A. Phenacenes: A Family of Graphite Ribbons. 2. Syntheses of Some [7]Phenacenes and an [11]Phenacene by Stilbene-like Photocyclizations. *J. Am. Chem. Soc.* **1997**, *119*, 2119−2124.
(39) Mallory, F. B.; Butler, K. E.; Berube, A.; Luzik, E. D.; Mallory, C. W.; Brondyke, E. J.; Hiremath, R.; Ngo, P.; Carroll, P. J. Phenacenes: a family of graphite ribbons. Part 3: Iterative strategies for the synthesis of large phenacenes. *Tetrahedron* **2001**, *57*, 3715−3724.
(40) Jolly, A.; Miao, D.; Daigle, M.; Morin, J.-F. Emerging Bottom-Up Strategies for the Synthesis of Graphene Nanoribbons and Related Structures. *Angew. Chem., Int. Ed.* **2020**, *59*, 4624−4633.
(41) Irie, M. Diarylethenes for Memories and Switches. *Chem. Rev.* **2000**, *100*, 1685−1716.
(42) Irie, M.; Fukaminato, T.; Matsuda, K.; Kobatake, S. Photochromism of Diarylethene Molecules and Crystals: Memories, Switches, and Actuators. *Chem. Rev.* **2014**, *114*, 12174−12277.
(43) Lvov, A. G.; Khusniyarov, M. M.; Shirinian, V. Z. Azole-based diarylethenes as the next step towards advanced photochromic materials. *J. Photochem. Photobiol., C* **2018**, *36*, 1−23.
(44) Rajeshkumar, V.; Courté, M.; Fichou, D.; Stuparu, M. C. Synthesis and Properties of Large Polycyclic Aromatic Hydrocarbons with Planar and Non-Planar Structural Motifs. *Eur. J. Org. Chem.* **2016**, *2016*, 6010−6014.
(45) Rajeshkumar, V.; Stuparu, M. C. A photochemical approach to aromatic extension of the corannulene nucleus. *Chem. Commun.* **2016**, *52*, 9957−9960.
(46) Halilovic, D.; Budanovic, M.; Wong, Z. R.; Webster, R. D.; Huh, J.; Stuparu, M. C. Photochemical Synthesis and Electronic Properties of Extended Corannulenes with Variable Fluorination Pattern. *J. Org. Chem.* **2018**, *83*, 3529−3536.
(47) Products of concivible photocyclization at C(7) and C(8a) positions were not observed. They are much less stable than **1a** and would require an oxidant to stablize the interediate.
(48) For details, see the Supporting Information.
(49) Melekhina, V. G.; Mityanov, V. S.; Lichitsky, B. V.; Komogortsev, A. N.; Lyssenko, K. A.; Krayushkin, M. M. Synthesis of Benzocarbazole Derivatives by Photocyclization. *Eur. J. Org. Chem.* **2019**, *2019*, 1335−1340.

https://dx.doi.org/10.1021/acs.orglett.0c01074
Org. Lett. 2020, 22, 3835−3840

(50) Cardona, C. M.; Li, W.; Kaifer, A. E.; Stockdale, D.; Bazan, G. C. Electrochemical Considerations for Determining Absolute Frontier Orbital Energy Levels of Conjugated Polymers for Solar Cell Applications. *Adv. Mater.* **2011**, *23*, 2367−2371.
(51) De Vleeschouwer, F.; Chankisjijev, A.; Yang, W.; Geerlings, P.; De Proft, F. Pushing the Boundaries of Intrinsically Stable Radicals: Inverse Design Using the Thiadiazinyl Radical as a Template. *J. Org. Chem.* **2013**, *78*, 3151−3158.
(52) We thank Referee for this comment.

https://dx.doi.org/10.1021/acs.orglett.0c01074
Org. Lett. 2020, 22, 3835−3840